Mine Water and the Environment (2024) 43:431–448
https://doi.org/10.1007/s10230-024-00998-y

TECHNICAL ARTICLE

Using Electrical Resistivity Tomography to Understand the Hydrogeological Behavior of Acid Drainage Percolation in a Fractured Aquifer at a Uranium Mining Site

César Augusto Moreira[1] · Leonides Guireli Netto[1,2] · Fernanda Miranda de Siqueira Buchi[1] · Marco Antônio Fontoura Hansen[3] · Henri Masquelin[4] · José Pedro Rebés Lima[3]

Received: 21 December 2023 / Accepted: 16 August 2024 / Published online: 2 September 2024

Abstract

Brazilian mining ventures aged 30 years or older were studied, revealing historical oversights in environmental planning that have caused substantial environmental liabilities during active mining and decommissioning. Electrical resistivity tomography surveys were conducted in a decommissioning uranium mine in southeast Brazil. The results provided valuable insights into local hydrogeological dynamics, revealing the flow of acid mine drainage in two distinct systems: the porous waste rock pile and the fractured underlying crystalline basement. Geo-electrical sections displayed conductive anomalies indicating hydraulic connectivity between the waste rock pile and the underlying fractured aquifer through crystalline basement fractures. This connection was substantiated by sub-vertical zones of low electrical resistivity interpreted as groundwater influx from the porous system to the fractured aquifer. Consequently, the waste rock pile acted as a localized recharge zone for the regional aquifer, facilitating chemical exchanges between the two systems. Furthermore, the study successfully differentiated less impacted saturated zones (resistivity ≈80 Ω·m) from those associated with acid mine drainage (< 40 Ω·m). Preliminary investigations identified a complex fracture network in the study area, comprising two main fault systems with preferential NE and NW orientations, nearly orthogonal to each other. This fracture network demonstrated continuity, playing a fundamental role in sustaining flow within the local and regional drainage network.

Keywords Environmental liability · Uranium mine · Waste pile · Aquifer · Electrical resistivity

✉ Leonides Guireli Netto
leonidesnetto@ipt.br

César Augusto Moreira
cesar.a.moreira@unesp.br

Fernanda Miranda de Siqueira Buchi
fernandabuchi@gmail.com

Marco Antônio Fontoura Hansen
marcohansen@unipampa.edu.br

Henri Masquelin
hmasquel@fcien.edu.uy

José Pedro Rebés Lima
jprebes@unipampa.edu.br

[1] Geosciences and Exact Sciences Institute (IGCE), São Paulo State University (UNESP), Rio Claro, São Paulo State, Brazil

[2] Cities, Infrastructure and Environment Department, Institute for Technological Research (IPT), São Paulo, Brazil

[3] Pampa Federal University, Caçapava Do Sul, Rio Grande Do Sul, Brazil

[4] Instituto de Ciencias Geológicas, Universidad de La Republica, Montevideo, Uruguay

Introduction

Mining and Environmental Liabilities: the Challenge of Acid Mine Drainage

Currently, the mining industry seeks to minimize environmental, social, and economic impacts through prior planning actions and direct and indirect investigations of the physical environment before, during, and after the end of operations (Gorman and Dzombak 2018; Islam and Murakami 2021; Owen et al. 2024). However, mining projects in Brazil that were 30 years old or more disregarded the environmental impacts of the activity in their planning phase, which has resulted in environmental liabilities at active mines and those in the decommissioning phase, with real challenges in terms of understanding and reducing impacts on soil and groundwater (Camarero et al. 2019; Koppe 2021).

Mining environmental liabilities essentially involve the construction of large pits or gallery systems to remove

hundreds of tons of soil and rock, along with the processing and disposal of materials with no economic value. These excavation and disposal structures alter hydrological and hydrogeological systems, with consequences for the general flow system and the quality of surface and underground water resources (Lyu et al. 2019; Moreira et al. 2022). Tailings dams or waste rock piles are the alternatives routinely used to dispose of materials with no economic value, in structures designed to be stable for many decades, especially in structural and geotechnical terms (Guedes et al. 2023; Guireli Netto et al. 2020; Nascimento et al. 2022). The set of minerals that make up the exploited deposits can be represented by economically insignificant quantities of reactive minerals under surface conditions, but sufficient to cause changes in the quality of water resources (Gomes de Oliveira et al. 2014). Sulphide minerals are particularly relevant in this scenario, as they oxidize when exposed to surface conditions, especially in regions with high rainfall, generating acid mine drainage (AMD) (Bowker and Chambers 2015; Placencia-Gómez et al. 2010).

This process occurs when oxygen, water, and microorganisms come into contact with sulphide minerals, mainly pyrite (iron sulphide) (Blowes et al. 2003). The low pH favours the dissolution of potentially toxic chemical elements associated with rock matrices (Akcil and Koldas 2006; Schoenberger 2016). As a result, these elements and other constituents of the rocks can leach into the groundwater, which contributes to the deterioration of local water quality (Nordstrom et al. 2015). Understanding the generation and percolation of the contaminant in the physical environment is necessary since acidic water reaching aquifers can adversely impact groundwater quality in areas close to mining operations.

Application of Electrical Resistivity Tomography in Mines in the Decommissioning Phase

In recent decades, the application of non-invasive methods, such as geophysics, in studies of environmental liabilities has been a very effective alternative, both in groundwater management and in the characterization, monitoring, and remediation of contaminated areas in porous or fractured aquifers (Jessop et al. 2018; Guireli Netto et al. 2023; Marques et al. 2021). Electrical resistivity tomography (ERT) is a non-invasive geophysical technique that enables rapid investigations of large areas in a manner, with low operating costs (Dimech et al. 2022; Martínez-Pagán et al. 2021). ERT has greater spatial coverage than the monitoring well meshes traditionally used in environmental investigation studies and can be used to detect inorganic contaminants in soil and groundwater (Anterrieu et al. 2010; Moreira et al. 2020). By measuring the apparent electrical resistivity of the physical environment, the technique has good sensitivity for detecting organic and inorganic compounds in aquifers and identifying electrically more conductive (or resistive, depending on the contaminant) zones that contrast with the values of the same parameter in the unaltered physical environment (Casagrande et al. 2019; Epov et al. 2017; Targa et al. 2019).

Particularly in studies of contamination from mining, the advantages of ERT over conventional groundwater monitoring, usually carried out by installing groundwater monitoring wells, are the ease of data acquisition, the high sample density, and the possibility of interpreting variations in electrical resistivity according to the hydrogeological context of the physical environment (Singha et al. 2015; Epov et al. 2017). In contaminated fractured aquifer systems, where the structural geological context conditions the migration and percolation of the contaminant in the physical environment, several studies have shown good results using ERT to define zones or preferential flow paths (Poisson et al. 2009; Oliveira et al. 2022; Almeida et al. 2023). In environments affected by AMD generation, the use of ERT enables the interpretation of acid water zones and the delimitation of the vertical and lateral extensions of the contamination plume, as well as its migration based on measurements of the electrical resistivity of the physical environment. Acosta et al. (2014) assessed the environmental risk of three reclaimed mining ponds using geochemical and geophysical techniques. ERT suggested the erosive process in two ponds, highlighting the need for overburden to reduce erosion and metal mobility. The immobilization of some metals in deposited materials was recommended, and the absence of discontinuities in the rock indicated a low risk of metal transport to deeper horizons. Cortada et al. (2017) analyzed the sealing of abandoned tailings ponds using ERT. The technique made it possible to assess the internal structure of the ponds, identifying wetter areas which were associated with leaks. Benyassine et al. (2018) studied a former lead mine using different electrical resistivity tests to identify pollution risks and trace contaminant pathways to groundwater. The results provided a thickness to the tailings material and rounded structures with high resistivity values in the center, suggesting potential pathways of metals in the fractures. Canales et al. (2020) carried out ERT and hydrogeological tests in a reclaimed tailings area and demonstrated the sensitivity of electrical resistivity to hydrogeological parameters, providing a reliable approximation of the distribution of water and saturation in the unsaturated zone.

In this study, ERT surveys were carried out at a uranium mine in southeastern Brazil during the decommissioning and environmental recovery phase, with the aim of evaluating the possible underground flow of AMD from the base of a tailings pile built by filling in a river valley. The results are relevant given the scarcity of ERT surveys carried out in mines during the decommissioning phase. While most studies of this type are conducted in operating mines, this

work focused on a critical phase in the lifecycle of a mine. In mines undergoing decommissioning, there is a pressing need for less costly investigation methods, as the mine no longer generates revenue and the allocation of financial resources is limited. In addition, the study is relevant because many mines can remain in the decommissioning phase for decades, resulting in a shortage of technical information on the structures built, such as tailings piles and dams, and on environmental monitoring practices.

Study Area

Location of the Study Area and Importance of the Uranium Mine

The study area is located in the northeastern part of the Osamu Utsumi Mine, which was the first uranium mine in South America and is located in the municipality of Caldas, in the state of Minas Gerais, Brazil. The site consists of the interface between a tailings pile and the AMD catchment. The tailings pile is mainly composed of capping material and waste rock with a concentration of < 170 ppm of uranium oxide (U_3O_8) (Leite 2010). A water retention pond has been installed at the base of the pile, that receives the acid effluents generated inside the tailings pond (Fig. 1). The uranium mine was commercially exploited in Brazil between 1982 and 1995, when the uranium ore was exhausted, and has since been in the process of decommissioning and environmental recovery (Souza et al. 2013). Currently, the mining sector is facing serious difficulties related to different environmental liabilities arising from mining activities, especially the generation of AMD, both in the tailings piles and in the mine pit (Fernandes et al. 1998; Franklin 2007).

Geological, Structural and Hydrogeological Context

The Osamu Utsumi uranium mine is located in one of the largest alkaline deposits in the world. The Poços de Caldas Alkaline Massif has an area of around 800 km^2, surpassed only by the 1300 km^2 alkaline massifs of the Kola Peninsula in Russia (Ellert 1959). The Poços de Caldas Alkaline Massif is made up predominantly of effusive and hypoabyssal rocks, plutonic rocks, and volcanoclastic rocks (Fig. 1). Phonolites are the predominant lithotype of the massif and cover ≈70% of the area. Subordinately, nepheline syenites, lujaurites, and volcanoclastic rocks are more commonly found in the northwestern part of the mining area. (Ellert 1959; Tedeschi et al. 2005; Zanlán and Oliveira 2005). The mineral assemblage of the lithotypes found in the Poços de Caldas Alkaline Massif basically consists of potassium feldspar, albite, sodium pyroxenes, nepheline, eudialite, biotite, and sanidine, as well as rare earth elements and concentrations of uranium and thorium (Ulbrich et al. 2002).

The genesis of the deposits is associated with the intrusion of a syenitic body into tinguaitic rocks and phonolites, with superimposed magmatic processes of deuteric and supergene hydrothermal alteration that occurred during the volcanic reactivation phase, which led to an intense concentration of metallic ores (sulphides), uranium and molybdenum minerals, as well as strong potassium enrichment in the rocks of the region. These processes also resulted in explosive activity that substantially affected the host rocks, giving rise to large packages of essentially volcanic breccias (Fraenkel et al. 1985; Capovilla 2001; Cipriani 2002). The uranium, molybdenum, and zirconium mineralization of the Poços de Caldas Alkaline Massif are concentrated in the central-eastern circular structure, highlighted by the geomorphology of the region. The typical mineralogical assemblage includes pechblende (U_3O_8), jordisite (MoS_2), sphalerite, zirconbaddeleyite (ZrO_2), fluorite, and pyrite (Schorscher and Shea 1992; Waber 1992).

The geological framework of the Osamu Utsumi uranium mine is characterized by the various rock types of the nepheline syenite class (tinguaites, phonolites, and foiaites), affected by volcanic and hydrothermal processes that have led to the formation of structural varieties, often found brecciated (Fig. 1) (Magno Júnior 1985). The Poços de Caldas Alkaline Massif has two main fault systems: the first, in a N60W direction, related to regional tectonics, and the second, in a N40E direction, resulting from the formation of the volcanic caldera (Fraenkel et al. 1985). Holmes et al. (1992) proposed the existence of a third subcircular fault system related to intrusions of the alkaline complex. The work by Targa et al. (2019) suggests that the fractures tend to follow the circular edges of the Poços de Caldas Alkaline Massif. In the northwestern portion of the alkaline massif, the regional fractures show a NE-SW trend. In the southeast, it is possible to see an intersection between two fracture systems, with trends to the NE and NW, almost orthogonal to each other. This structural context controls the hydrogeological behavior of the area. The groundwater of the uranium mine is contained in a porous aquifer system formed by the tailings piles, which are superimposed on the regional fractured aquifer system formed by the crystalline basement (Fernandes and Franklin 2001). Underground flow in this environment is quite complex and essentially conditioned by structures such as faults and fractures. The drainage network of the Poços de Caldas Alkaline Massif is conditioned by the morphostructural pattern of the region, with a dendritic or sub-parallel pattern associated with the dense fracturing of the rocks. The study region is characterized by fractured aquifers, which are marked by strong anisotropy and heterogeneity, depending on the scale of work adopted

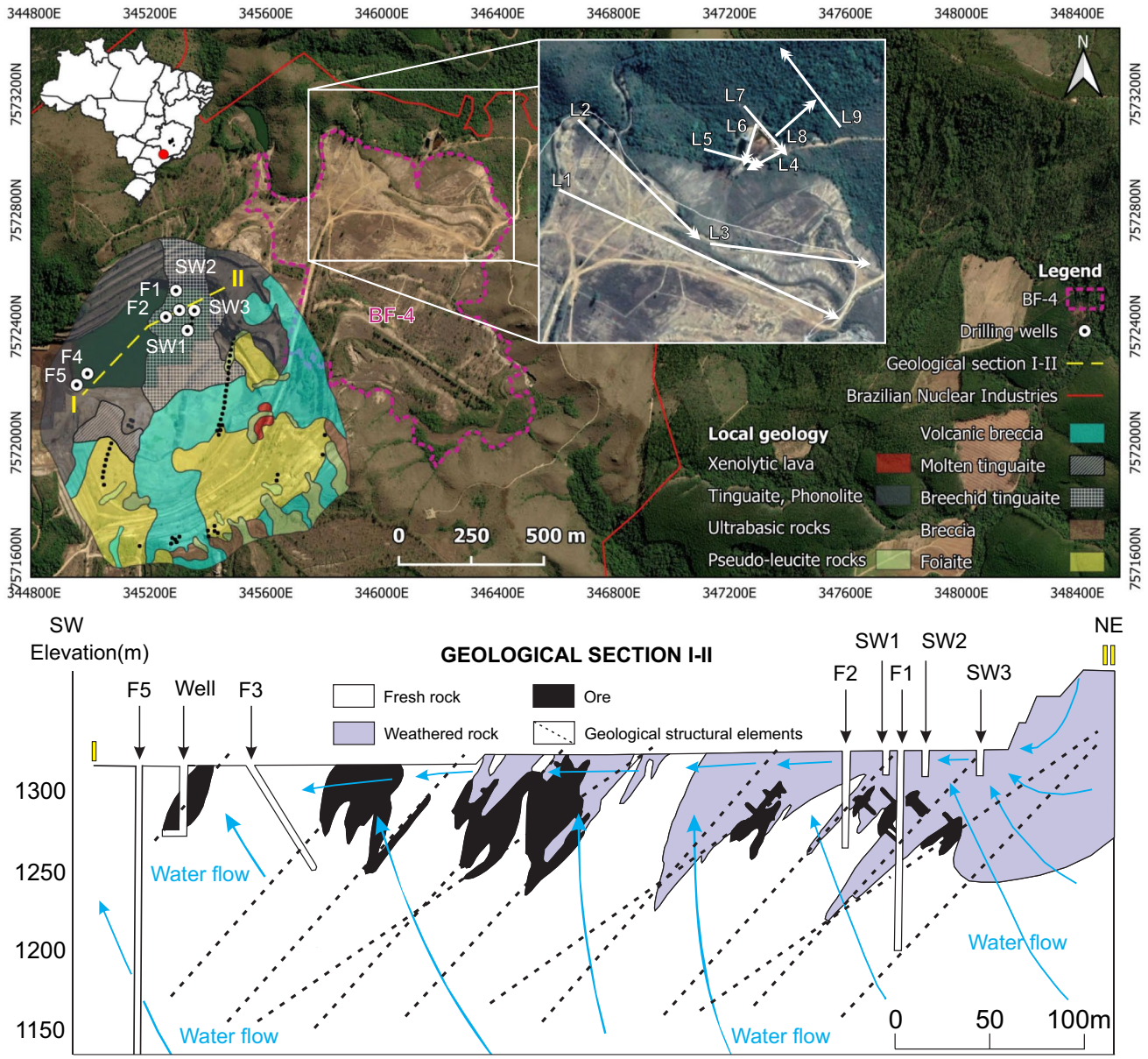

Fig. 1 Location of the study area with details of the hydrogeological mapping conducted in the mine pit and the positioning of geophysical acquisition lines in the mining waste pile area

(Gudmundsson et al. 2003). The main water-transmitting zones in these systems consist of secondary structures of a tectonic or anthropogenic nature, such as joints or fractures (Fernandes et al. 2022). Studies by Fagundes et al. (2008) and Lachassagne et al. (2001) also point to weathering processes as agents that promote secondary porosity in the crystalline rocks through the formation of alteration mantles and the dissolution of minerals in the rock matrix. Groundwater flow in these environments is linked to the density, connectivity, and openness of the fractures (Fernandes et al. 2022).

Tailings piles, in turn, are granular/porous aquifer systems, due to their high variability in particle size (Franklin 2007). The material removed from the pit was deposited in tailings piles located in the valleys and adjacent slopes, which resemble porous aquifers in which the coarse granulometry of the tailings results in a high percentage of macropores and, consequently, a low percentage of small pores, which provides high permeability (Cipriani 2002). Once the tailings piles were built, they became part of the local hydrological system subject to rainwater infiltration and the influence of local water bodies, as well as seasonal run-off (Franklin 2007). The mine's porous aquifer system

is also made up of the weathered mantle resulting from the alteration of the outcropping rock matrix in the area and favoured by the region's humid climate. Thus, the hydrogeological context of the Osamu Utsumi uranium mine area can be characterized by the presence of a mixed aquifer system, represented by a porous/granular aquifer (corresponding to the tailings piles and the mantle of rock matrix alteration) superimposed on a fractured aquifer system, formed by the crystalline basement (Fig. 1). According to the work of Holmes et al. (1992), the Osamu Ustumi mine affected the local groundwater dynamics by modifying the original topography of the land as well as by the consequent lowering of the local phreatic surface and disturbances in the groundwater flow patterns, such as the construction of the tailings piles.

Environmental Liabilities Arising from Mining Activities

The reserves contained in the region where the Osamu Utsumi mine is located have been estimated at ≈17,200 tons of uranium oxide (U_3O_8), with open-pit mining (Fraenkel et al. 1985). The operational process at the Osamu Utsumi mine was divided into three stages: mining, physical processing, and chemical processing. The defined cut-off grade was 170 ppm of soluble uranium. The material generated in the blasting of the mine, characterized as waste (values below 170 ppm of U_3O_8), was sent to places defined as dumps (Cipriani 2002). Around 2.39×10^6 m^3 of tailings were produced during the mine's years of operation (Franklin 2007). The tailings dump targeted by this study covers an area of 56.9 ha and contains 12.4 million m^3 of waste material, arranged in two levels, upper and lower. It has about 70 m of slope, with an inclination of 70° (Cipriani 2002).

The material used to build the pile comes from blasting and mining the ore body (Cipriani 2002), the lithology of which is made up of volcanic breccia and phonolite (Magno Júnior 1985; Franklin 2007; Pelisam 2020). Mineralogical analyses of the outcrop, carried out by Pelisam (2020) using total powder x-ray diffractometry, indicated that the majority components of the volcanic breccia are alkali feldspars (microcline/orthoclase) and potassic phyllosilicates (illite/sericite), the combined quantities of which exceed 80% of the rock's total mineralogy. Secondary accessory minerals were identified, such as albite and nepheline. Pyrite, a mineral associated with the process of generating AMD, was detected in small quantities, around 1.1% of the rock's total. The mineral is fine-grained, less than 100 µm, which gives it intermediate chemical reactivity (Pelisam 2020). The material from the blasting process was deposited on the upper level of the pile, while the tailings produced by the sorting of the ore body were disposed of on the lower level (Alberti 2017).

The tailings were disposed of in the open by filling in the old valley, the bed of which was diverted to the side of the pit in order to channel the water downstream from the pile (Cipriani 2002). However, the work of Nascimento et al. (2022) indicates that stream water continued to infiltrate into the pit. The pile was built using the descending method, so that the finer material is concentrated at the top of the pile and the coarser particles are mostly placed at the bottom (Franklin 2007). At the base of the main slope of BF-04, groundwater affected by the AMD process emerges in the midst of boulders. A water catchment pond, called the BNF, was installed downstream of the pile to receive the acid effluent generated inside the tailings pile (Fig. 2).

Initially, the retention pond had no waterproofing. Subsequently, the current pond was built with a waterproof blanket, which was moved to the side of the old pond to reduce the infiltration of acidic water into the soil and aquifer. However, water still accumulates in the old pond, which has contributions from BF-04 via fractures and rainwater (Fig. 3). The water retained in the pond is pumped to the mine pit through pipes, where it is mixed with the water drained from the pit. Afterwards, the effluent stored in the pit is pumped to an effluent treatment plant, where hydrated lime is added to make the necessary pH corrections and precipitate and remove metals and radionuclides (Cipriani 2002). It is estimated that 2,500,000 m^3 of water are treated per year, with consumption of 3,500 tons/year of hydrated lime, in addition to the generation of around 20 tons of uranium oxide (U_3O_8) in the form of calcium diuranate, resulting from the treatment of acidic water (Cunha et al. 2015).

Materials and Methods

Electrical Resistivity Tomography (ERT)

Apparent electrical resistivity values of the subsoil were acquired using the ERT technique by installing electrodes on the surface of the soil. A pair of electrodes are used to inject electric current into the subsoil, while other electrodes are used to measure the resulting electric potentials (Ward 1990). These measurements are then used to calculate the electrical resistivity distribution of the subsoil. The fundamental ERT formula is Ohm's law, which describes the behavior of electrical current and electrical potentials in the subsoil. The process involves applying an electric field via current electrodes and measuring electric potentials on potential electrodes. The fundamental equations are derived from Ohm's law and the electric current continuity equation. The expression is given by Eq. (1):

$$V = IxR \tag{1}$$

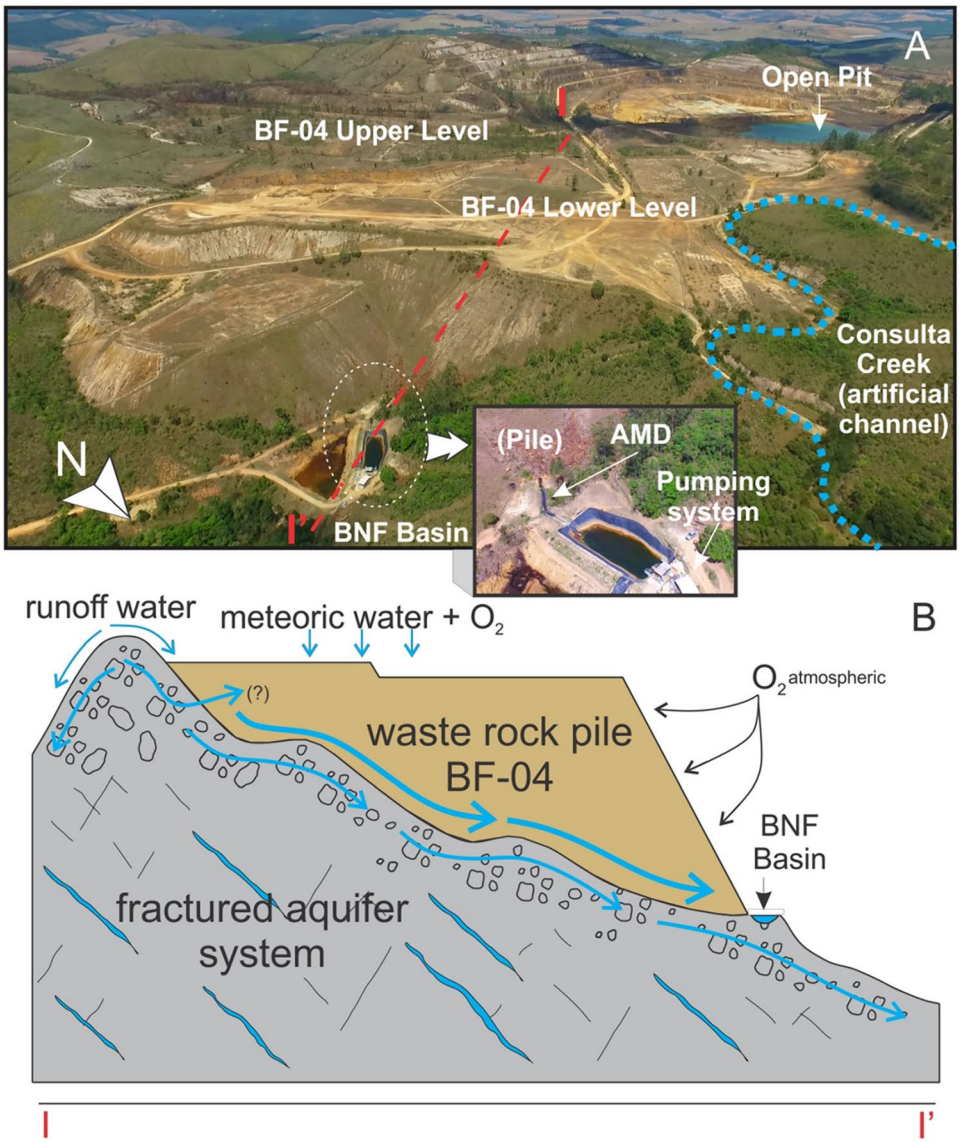

Fig. 2 Overview of the waste rock pile, detail of the AMD emergence at the base of the pile, and the collection retention ponds, with a schematic section of the aquifer systems present in the Osamu Utsumi mine (modified from Casagrande et al. 2019)

when applied to the subsoil, where V represents the potential difference measured between two electrodes, I is the current injected, and R is the resistance, which depends on the distribution of electrical resistivity in the subsoil. The apparent electrical resistivity values obtained during data acquisition are processed in dedicated software using geophysical inversion equations (Loke and Lane Jr 2004). The aim is to invert the electric field equations to obtain the resistivity distribution from the electric potential measurements. The inversion techniques use algorithms to iteratively adjust the resistivity models until the differences between the measured and calculated values are minimized (Binley 2015). The difference between the apparent values calculated and measured in the field and those obtained by the block model is expressed by the root mean squared (RMS) error.

In this study, the ERT was established at the interface between the waste rock pile and the AMD retention pond at the Osamu Utsumi mine. The goal was to understand the local hydrogeological dynamics and the regions with the greatest volumes of AMD, based on the characterization of contrasts in the intrinsic properties of the materials (electroresistivity), as a result of the alteration of the physical properties of the natural environment by the contaminants. The equipment used in the field was an ABEM Terrameter LS resistivity meter (84 channels, 250W, with a resolution of 1 μV and a maximum current of 2.5A) (ABEM 2012), connected to a battery. The equipment allows automatic acquisitions by means of a preliminary configuration. The configuration parameters used in this work were: 1A of current and an acquisition time of 1.5 s. The electrodes used were metal. The geophysical data was acquired in three campaigns, carried out in April, June, and October 2021, after occasional rainfall in the region. Nine acquisition lines and one reference line for the values

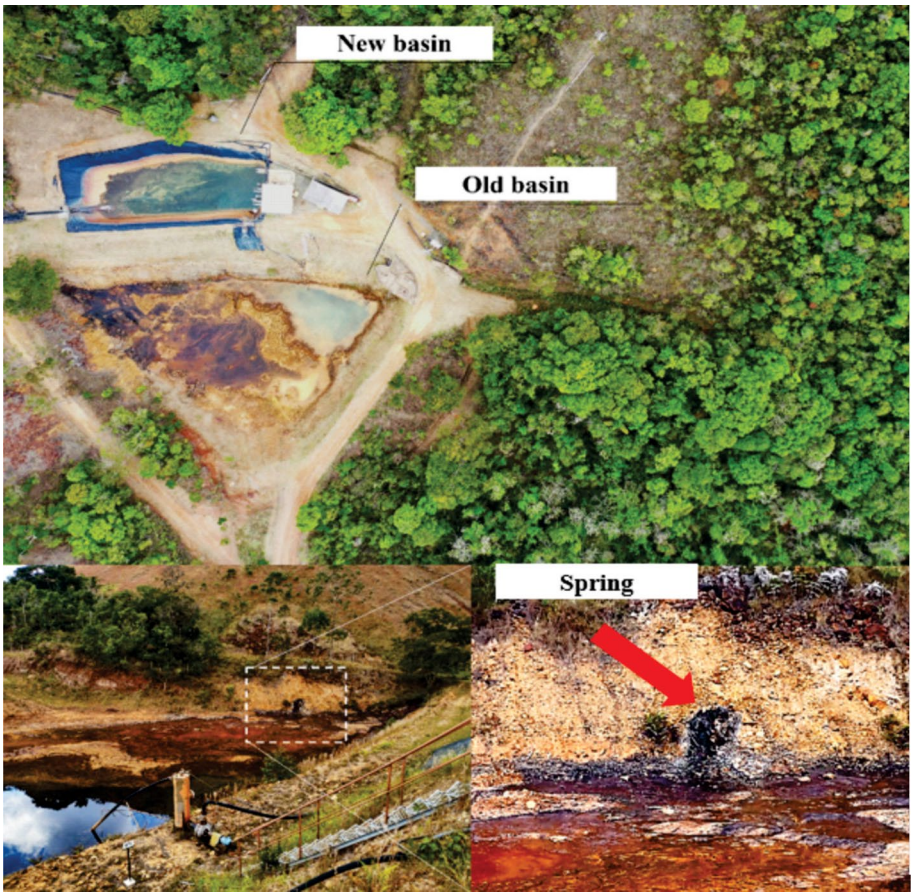

Fig. 3 Old and current catchments. Detail of the positioning of AMD on one of the slopes of the old catchment

obtained were defined. Acquisition lines 1 to 3 were located on the upper level of BF-04, while lines 4 to 9 and the reference line were positioned downstream of it, in direct contact with the bedrock, downstream of the tailings pile, in the water catchment pond area (lines 4 to 7), and in an area with native vegetation (lines 8 and 9). The spacing between electrodes varied from 3 to 5 m (lines 1 to 3, lines 4 to 9, and reference, respectively), depending on the depth of investigation stipulated for each line. The length of the lines also varied: line 1 was the longest, at ≈600 m, and line 8 was the shortest, at ≈100 m, so that the geophysical tests were deep enough to allow analysis of the fractured aquifer beneath the pile.

Two geoelectric arrays were used: Schlumberger (lines 1 to 3 to highlight the boot contact zone and the underlying fractured bedrock, and dipole–dipole (lines 4 to 9), to highlight the bedrock fractures and any flow paths (Fig. 4). The use of different geoelectric arrays, such as Schlumberger, dipole–dipole, and others, in ERT studies plays a crucial role in obtaining more comprehensive and accurate information about the properties of the subsurface (Moreira et al. 2016). Each array has specific advantages that can be exploited to meet different research objectives. The Schlumberger array, for example, is effective for exploring deeper layers, while the dipole–dipole is more sensitive to near-surface features. Variations in electrode array influences the sensitivity of the method to different types of subsurface, such as fractures, layer interfaces, and saturation zones. By employing various arrays, it is possible to increase the likelihood of detecting and characterizing a variety of geological features (Binley 2015; Moreira et al. 2016).

The ERT data was tabulated along with the geographical coordinates and altitude of each point. The data acquired in the field was processed using Res2Dinv software, version 3.53 (Geotomo Software), to generate two-dimensional sections with resistivity values based on the distance from the origin of the line and the depth of acquisition. The software interpolates and inverts the field data using the Least Squares method. This technique smooths out extreme values to achieve better compatibility between the theoretical model and the data collected in the field (Reynolds 2011; Binley 2015). The resistivity inversion models required five to seven iterations to obtain reliable results, as indicated in each 2D section. The earth's subsurface is recognized by the program as rectangular blocks that have constant values for the parameter under investigation, which can then be adjusted based on field measurements. The topographic values of each electrode were also entered to configure the relief (Loke and Baker 2004). The

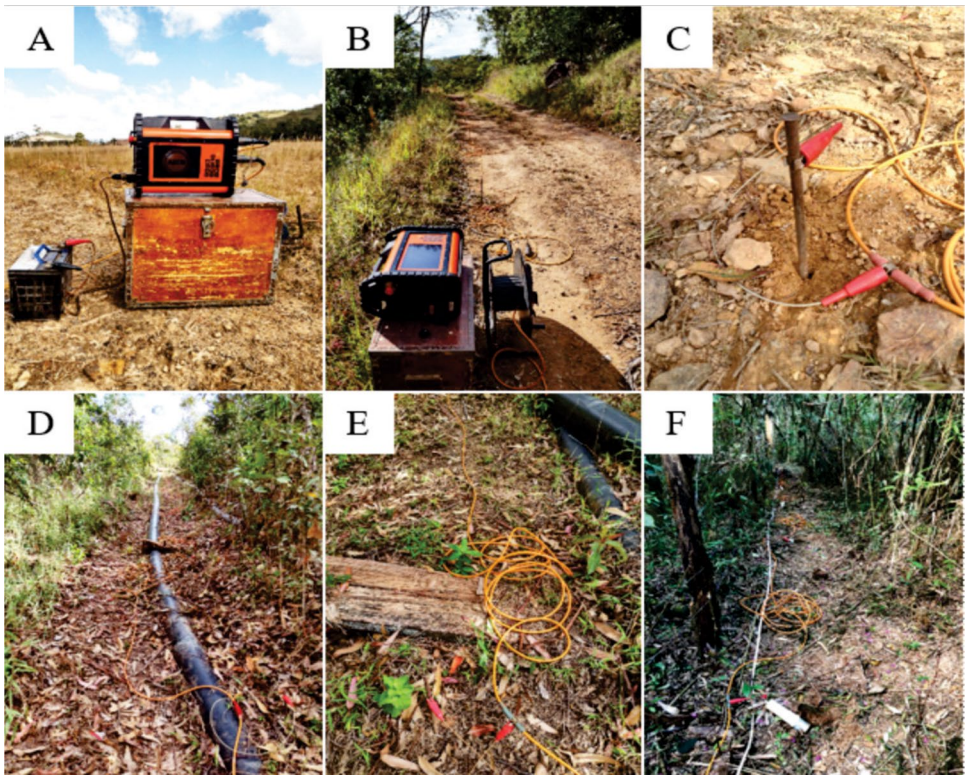

Fig. 4 Data acquisition: **A** Terrameter resistivity meter connected to battery; **B** Terrameter resistivity meter and set up geophysical line; **C** Metal electrode; **D E F** Set up geophysical lines

final data is presented in the form of 2D sections, based on the conversion of the measured values into a synthetic model of the parameter. The chromatic representations adopted in this work for the resistivity data are warm tones for high electrical resistivity indices and cool tones for lower electrical resistivity indices. The steps taken to obtain the 3D models of the contamination plume followed the same principles as those used in mineral prospecting, using the Oasis Montaj platform (Geosoft), in which the spreadsheet files were uploaded and the data relating to the sections were interpolated using the kriging method, followed by minimum curvature, making it possible to smooth out the central values to the detriment of the extremities. The sampling mesh used, together with statistical criteria, established different blocks for each point in the final 3D model, which made it possible to generate maps for different depths.

Results and Discussions

The ERT Reference Line

The resistivity inversion models representative of the study area were presented on a logarithmic scale of values ranging from 20 Ω·m to 2000 Ω·m. The maximum depth reached by the tests was 120 m, so that the entire thickness of the waste rock and the alkaline rock foundation was covered during data acquisition, since the maximum height of the mining waste pile is ≈70 m at the front, closest to the slope. The reference line showed the natural electrical resistivity pattern for the area, since it is located in a strategic place, far from the tailings piles and therefore without interference from contaminants. The presence of AMD in the geological environment alters the electrical properties of the aquifer and the quality of the groundwater in places where acid effluents percolate, which leads to a reduction in resistivity values due to an increase in salinity, a physical–chemical property characteristic of AMD (Akcil and Koldas 2006). The reference line showed values > 1036 Ω·m along the entire surface, reaching a depth of 6 m, indicative of dry soil. From 10 m, a decrease in resistivity values was observed, which indicated the presence of rock/soil with a moderate degree of saturation. The section showed a saturated zone, located on the left, evidenced by resistivity values of ≈74.6 Ω·m. Values of 20 Ω·m to 74.6 Ω·m suggested the presence of water with a variable amount of dissolved ions, referring to regions affected by the process of generating AMD, the object of interest in this work (Fig. 5). Several studies have demonstrated the geoelectric signature of low electrical resistivity (< 74.6 Ω·m) of soil and groundwater impacted by AMD (Li et al. 2015; Targa et al. 2019; Moreira et al. 2020). Values closer to 20 Ω·m indicate a greater amount of dissolved salts, while values closer to 74.6 Ω·m denote a lower concentration of these elements, analogous to the resistivity values expected for natural groundwater.

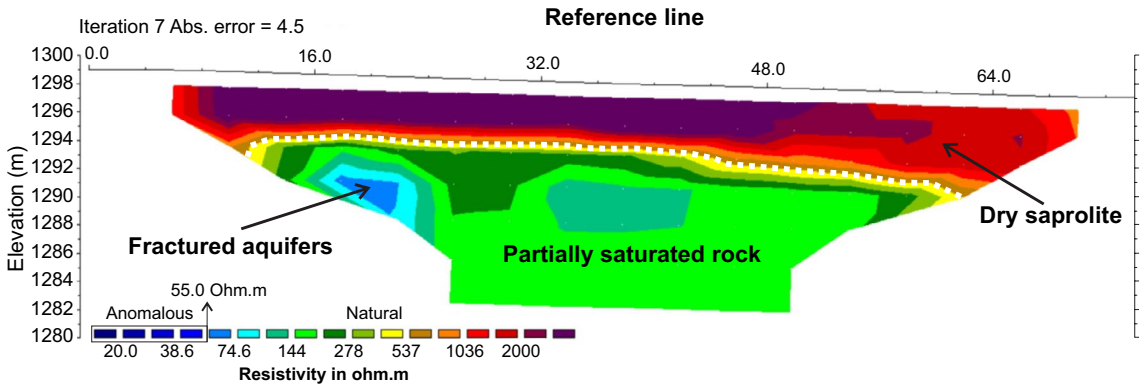

Fig. 5 ERT reference line and interpretations of electrical resistivity anomalies related to different geological elements: saprolite, partially saturated rock, and fractured aquifer

Values between 74.6 Ω·m and 144 Ω·m refer to sites with a moderate degree of saturation. Intervals above 144 Ω·m indicate a low degree of saturation for both the rock mass composed of alkaline rocks and the materials that make up the tailings pile.

ERT Acquisition Lines Conducted over the Mining Waste Pile

Lines 1, 2, and 3 showed a very similar distribution pattern of electrical resistivity values, with the presence of a continuous zone of low resistivity along the entire length of the geophysical lines (Fig. 6). The layer can be interpreted as a saturated zone, and begins at a depth of 1380 m to a depth of 1340 m, with a thickness ranging from 10 to 40 m. It is likely that this shallow saturated portion is related to meteoric water contributions from recent rainfall at the site. This configuration can be explained by the process of material deposition and the physical characteristics of the constituent rock materials. The construction of BF-04 took place by advancing the tip of the embankment and, consequently, without controlling and compacting the dumped material, which led to great granulometric heterogeneity of the tailings that make up the tailings pile (Franklin 2007). Consequently, the granulometric segregation inside the tailings pile is mainly due to gravitational action, so that the finer material is concentrated at the top and the coarser granulometries go deeper, as demonstrated by Anterrieu et al. (2010) and Franklin (2007). In this way, water infiltration at the top of the pile occurs slowly, while there is rapid dispersion at greater depths. Another factor that influences the hydraulic behavior of the tailings pile is the degree of compaction of the materials used to form the pile. The trajectory of heavy equipment over the pile, such as excavators and tractors, accentuates the compaction of the finer waste, which results in dense, horizontal layers in the middle of coarser sections. Places with a high degree of compaction show a reduction in the size and quantity of conductive pores and, consequently, less capacity to disperse effluents. This configuration can be seen in the central portion of Line 2, which showed a less resistive layer, with resistivity values of ≈100 Ω·m, located between 1360 and 1350 m, in a low resistivity environment. In view of this, it is expected that the hydraulic conductivity in the superficial part of the pile is less than in its base, which generates preferential flow paths inside the pit, corroborated by the 2D models evaluated.

Another feature observed in Sects. 1 to 3 was the existence of a continuous zone of high resistivity (> 300 Ω·m), located at the base of the sections, at a depth of ≈60 m. This portion was interpreted as the slightly weathered/fractured crystalline bedrock, marked by the change from a saturated zone with high porosity to a region with little or no water percolation. The results for the bedrock are not in the same electrical resistivity range as the partially saturated part of the reference line. This is because the reference line was carried out outside the area of possible influence of AMD. As a result, the electrical resistivity values for the rock were different from those observed in the ERT sections carried out inside the mine. It is possible to interpret that the saturated zone observed in Sects. 1 to 3 is contained in the granular system (formed by the tailings pile) and is limited by the contact interface between the base of the pile and the massive crystalline basement. In short, the crystalline basement limits the infiltration of water due to its impermeability and leads to the accumulation of groundwater at greater depths. In Sects. 2 and 3, vertically shaped saturated zones were identified in the central portion of the outcrop, at a depth of 30 m (marked by the dotted arrow in Fig. 6). These zones seem to have continuity at deeper levels, probably beyond the interface of the contact between the base of the tailings pile and the crystalline bedrock, which suggests the occurrence of infiltration and transportation of acid effluents into the fractured aquifer from the granular aquifer system, through fractures. Electrical anomalies allow us to interpret

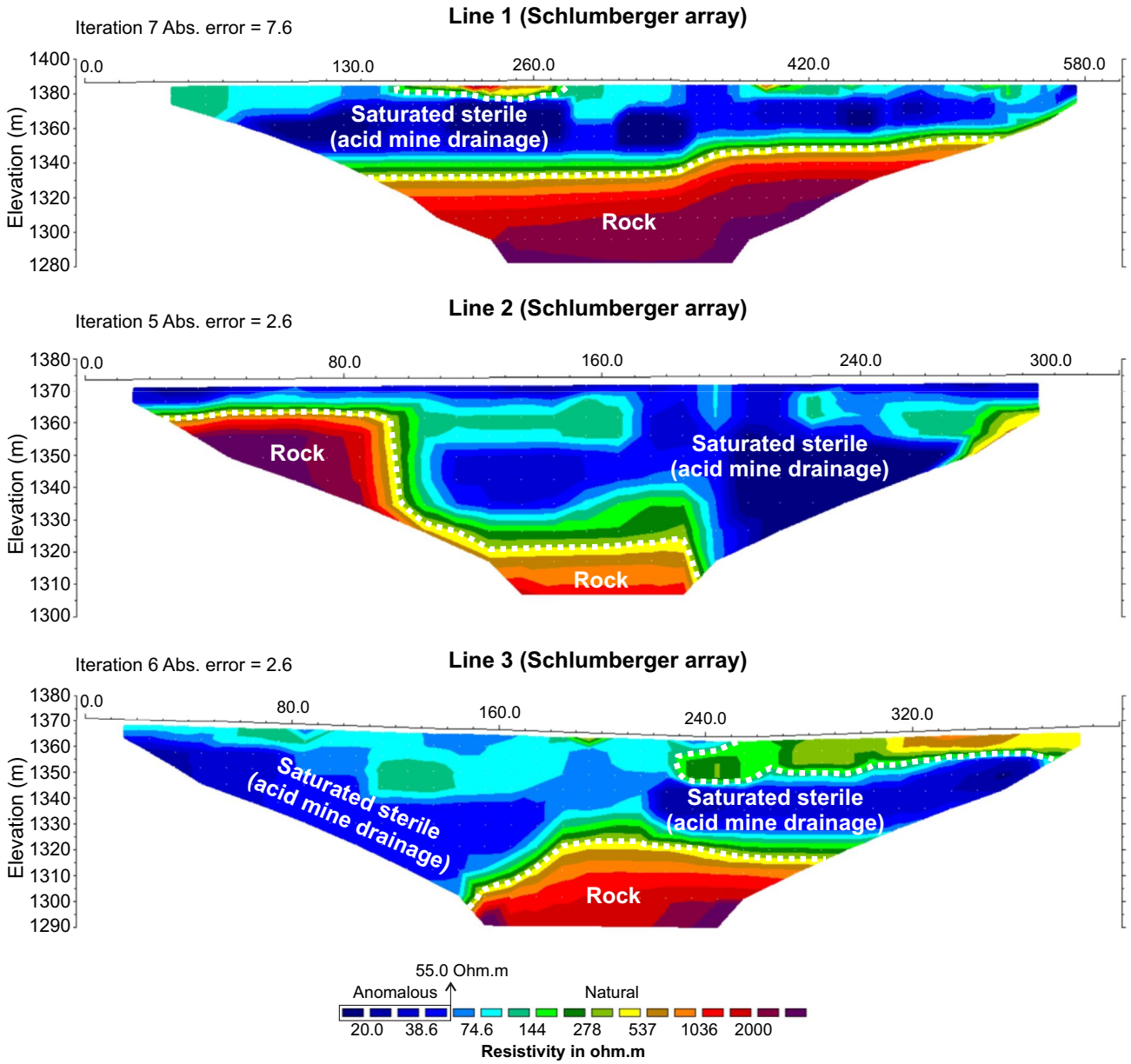

Fig. 6 Resistivity inversion models related to acquisition lines 1 to 3. The dashed white lines delineate the electrical anomalies of interest

that water accumulated at the base of the pile contributes to the fractured aquifer. From a hydrochemical point of view, in general, all the sections showed regions with lower electrical resistivity values, on the order of 20 Ω·m, probably due to the high salinity caused by the presence of AMD. These less electrically resistive cores are probably associated with regions with a higher concentration of residual sulphide material. The electrical resistivity of the soil is influenced by various factors, including moisture, mineralogical composition, and the salinity of the water present in the soil pores. In the presence of acid mine water, with a high concentration of contaminants, there is a marked change in soil salinity. This increase in salinity causes a decrease in the soil's electrical resistivity. Recent geoelectric studies have obtained electrical resistivity values consistent with those found in this study (Moreira et al. 2020; Dimech et al. 2022; Ali et al. 2023).

ERT Acquisition Lines Conducted at the Base of the Mining Reject Pile

The ERT lines carried out near the base of the waste rock pile with a NW–SE orientation were lines 5 and 7. Line 5 showed two electrical anomalies interpreted as zones saturated with acidic water (< 20 Ω·m) located in the central portion. The conductive values and geometry of the anomalies suggest the continuity of the groundwater flow observed in the Line 2 result (Fig. 7). The electrical anomaly was in a northeasterly direction, in line with the natural drainage system of the study site. This information is essential for understanding how acidic water is moving through the area, making it possible to identify possible contamination routes and hotspots. Line 7 is positioned perpendicular to BF-04, downstream of the water catchment pond. It was possible to observe the presence of a horizontal electrical anomaly with an initial depth of 10 m and a distance of 50 m and 70 m from the origin of the line, evidenced by resistivity values ranging from 20 to 40 Ω·m (Fig. 9). These zones can be interpreted as an interception of the groundwater flow coming from the tailings pile and percolating through the fracture system of the crystalline basement, suggesting that there is effluent flow downstream from the water catchment pond region. Understanding the extent of metal-rich water contamination and its potential influence on surrounding areas is crucial for determining the best environmental remediation techniques. Understanding the dynamics of the underground flow contributes directly to the development of preventive and corrective measures aimed at minimizing the environmental impacts associated with this form of contamination. In this way, the results obtained in lines 5 and 7 helped interpret and understand the results obtained in the lines carried out further downstream from the pile, at lower topographic levels (lines 8 and 9).

The ERT lines carried out near the base of the tailings pile with a NW–SE orientation were lines 4 and 6. Lines 4 to 6 were positioned near the foot of BF-04, in the region of the mine's water catchment pond, which is designed to store the water flowing from the base of the tailings pile and pump

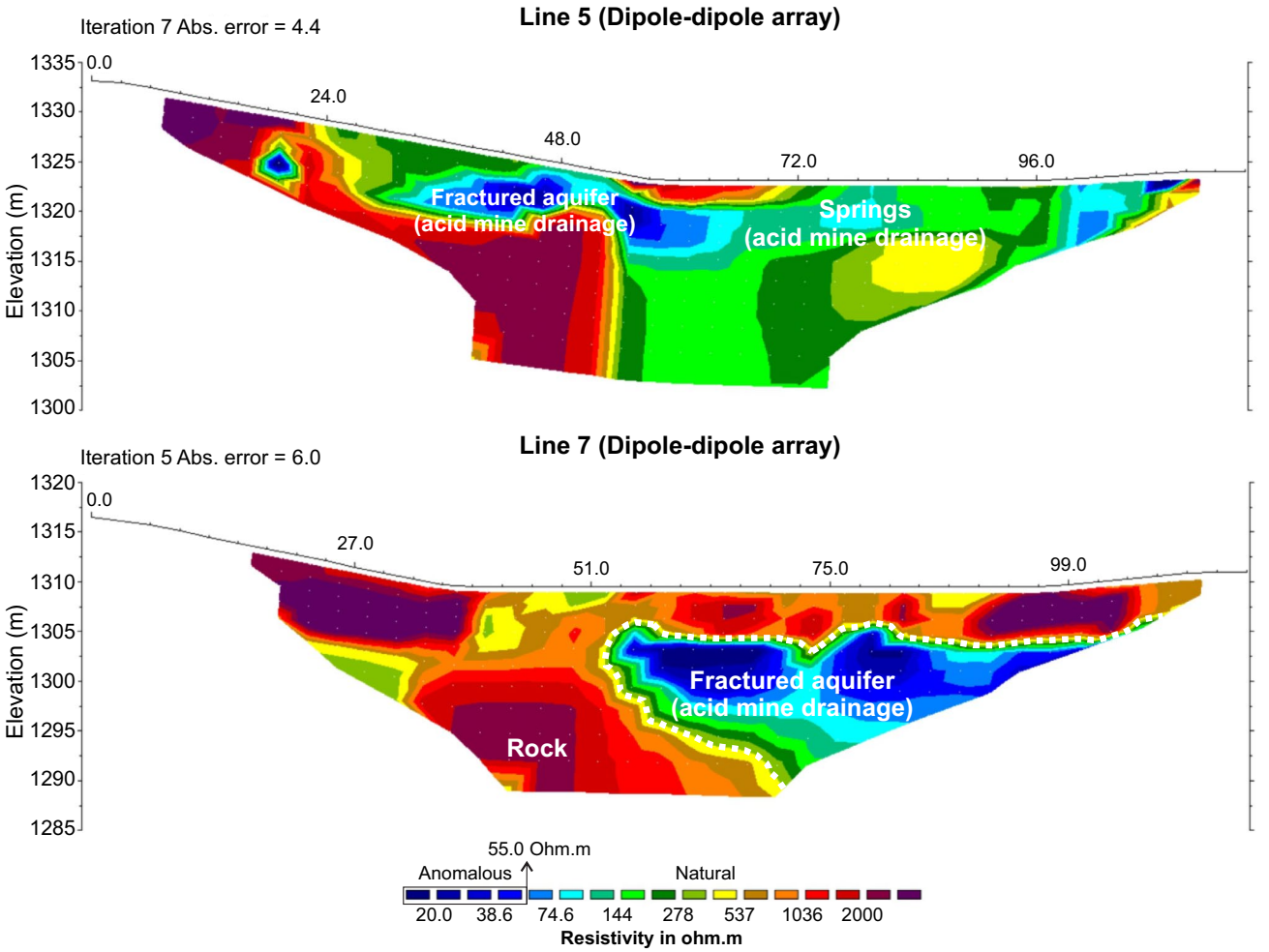

Fig. 7 Inversion models of electrical resistivity related to acquisition lines 5 and 7. The white dashed lines outline the anomalies of interest

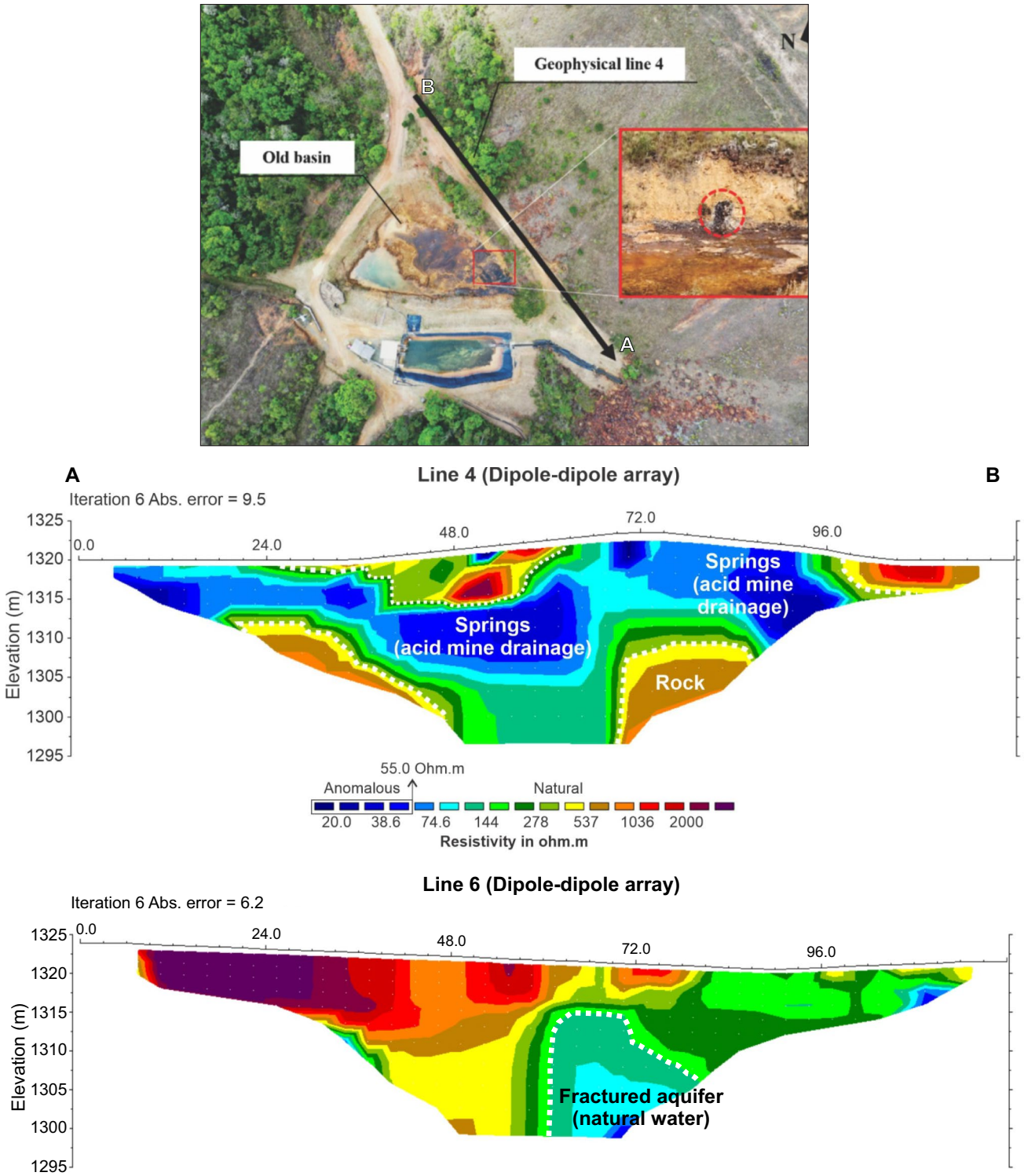

Fig. 8 Detailed positioning of acquisition line 4 with emphasis on the point of AMD upwelling in the inversion model and ERT line 6 and interpretations of electrical anomalies related to fractured aquifer

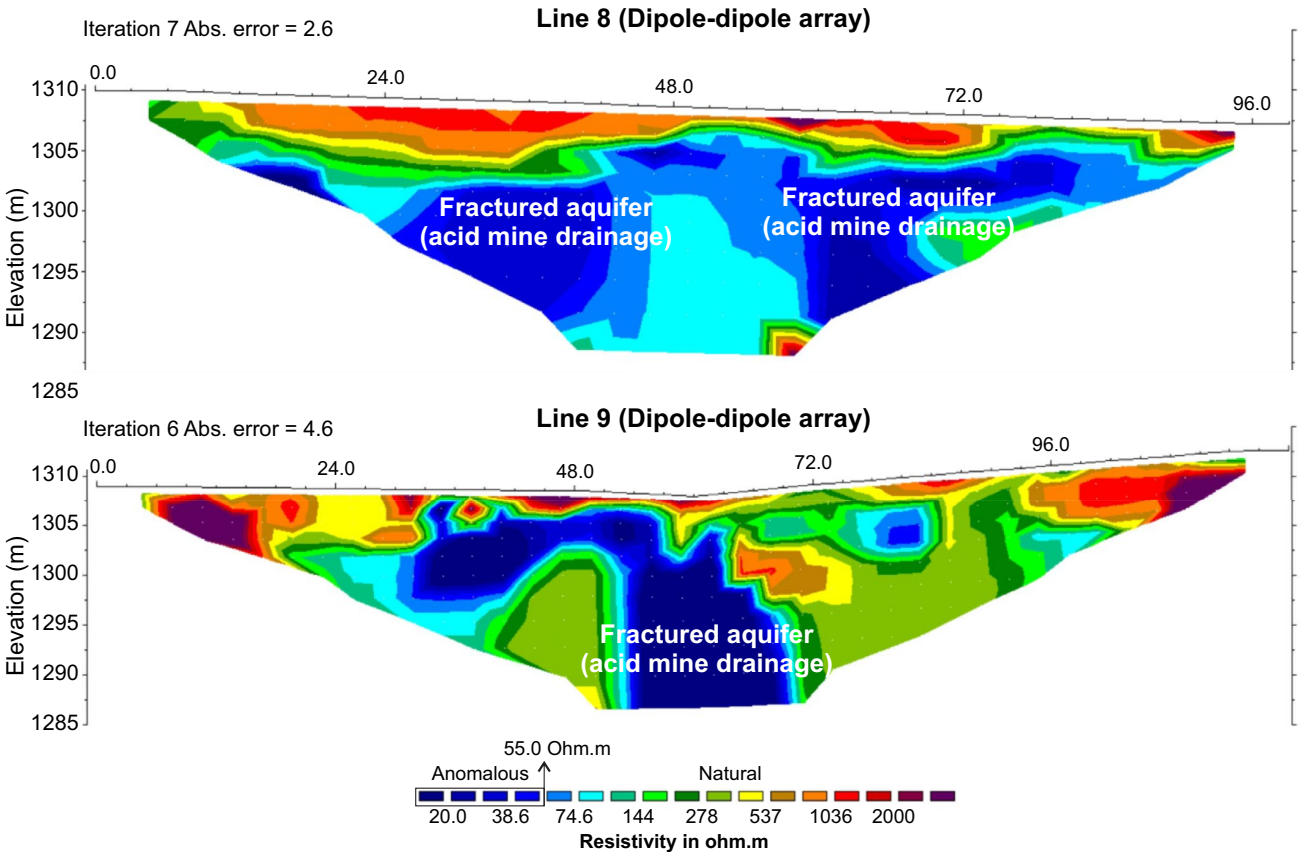

Fig. 9 Inversion models of lines 8 and 9 conducted further away from the mining waste pile downstream. Emphasis on the area with electrical anomalies suggesting AMD flow in this location

it to the effluent treatment plant. It is important to note that, topographically, there is a gradient of around 70 m from the top of the tailings pile. The region investigated in lines 4 and 5 corresponds to the boundary between the base of the tailings pile and the bedrock. Line 4 is 115 m long and 30 m deep and is located upstream of the old water catchment pond. The analysis of Sect. 4 showed electrical anomalies that suggest the migration of acid effluents through the fracture system of the crystalline basement, evidenced by two vertically saturated zones with resistivity values of around 20 Ω·m, located in the central portion and at the left end of the section (Fig. 8). These zones showed the continuity of the groundwater flow observed in line 3, heading north and northwest, respectively. The data from the inversion model was corroborated by field evidence, as fracture emergences were observed in the old water catchment pond (Fig. 8). Line 6 also showed the same configuration of electrical resistivity values as the sections described above, where it was again possible to observe electrical anomalies that suggest the input of acidic water through the crystalline basement fracture system (Fig. 8).

ERT Acquisition Lines Conducted Downstream of the Mining Waste Pile

Lines 8 and 9 were laid out in a topographically lower region than the other ERT lines, with extensive vegetation, and located downstream from the water catchment pond area. It is also important to note that line 8 was oriented perpendicular to the other acquisitions. Analysis of Sects. 8 and 9 also revealed electrical resistivity values of ≈20 Ω·m, which suggest the presence of acidic water zones in the area under investigation. The electrical anomalies were vertical in shape, located in the central portions of the sections and reaching deeper levels, which is indicative of percolation through fractures, with lateral continuity confirmed by Sect. 8 (Fig. 9). The geophysical models showed that although the water catchment pond captures the acidic water from the base of the BF-04 pile, part of the effluent flows downstream through the fractures in the crystalline basement and contaminating the local fractured aquifer.

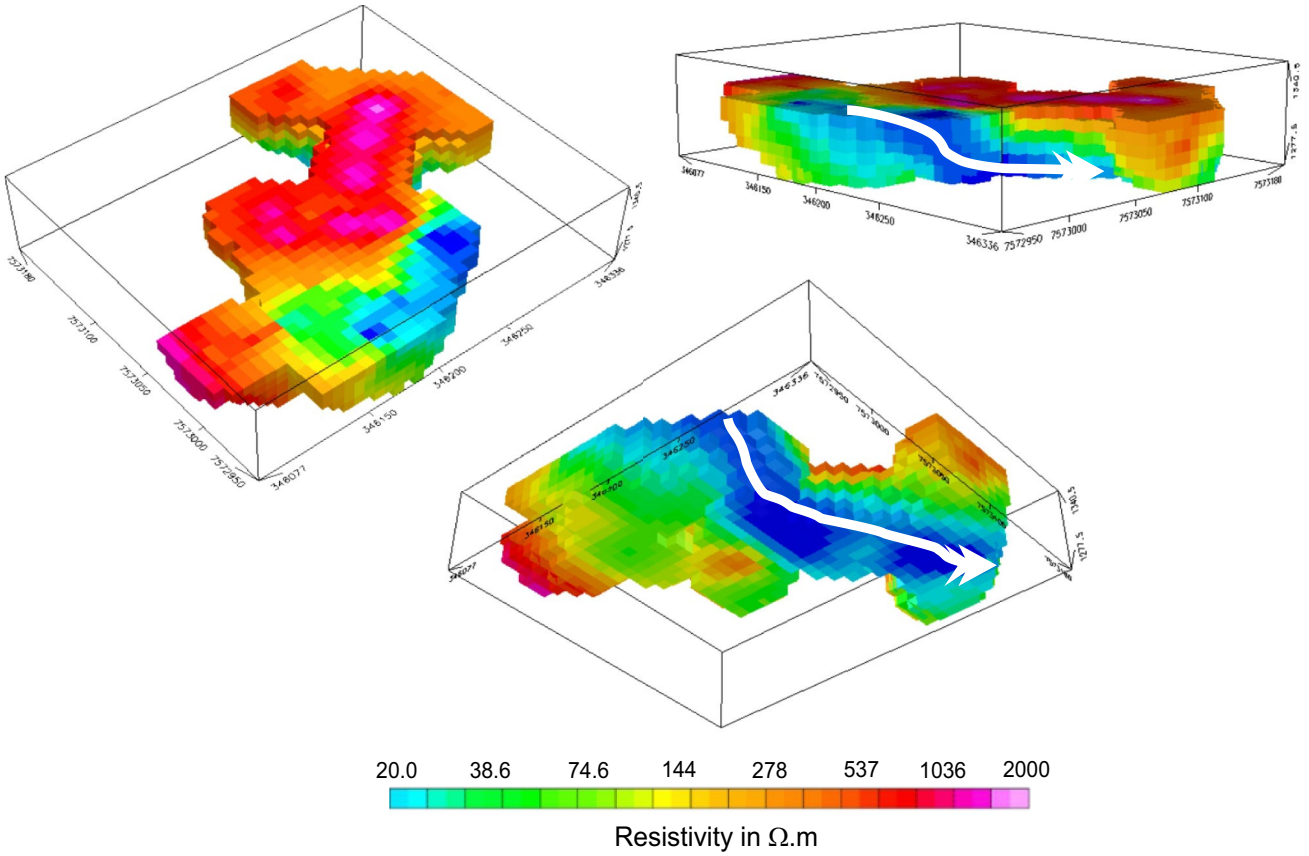

Fig. 10 3D visualization models of electrical resistivity, highlighting the development of electrical anomalies in depth, suggesting a preferential zone for AMD flow (marked by the white arrow in the models)

Three-dimensional Electrical Resistivity Models Obtained by Interpolating the 2D ERT Lines

The interpolation of geophysical Sects. 4 to 9 enabled the generation of 3D visualization models for the physical parameter of electrical resistivity representative of the area evaluated (Fig. 10). The choice of the sections to be used was based on the altitude of the electrical tomography lines, in view of the topographic unevenness in the region evaluated, and prioritized the characterization of hydrogeological flows occurring in the bedrock.

The images were smoothed and 11 depth levels were defined. The depth levels correspond to elevations of 1335 m (surface), and 1330, 1325, 1320, 1315, 1310, 1305, 1300, 1295, 1290, and 1285 m. The ground surface considered by the pseudo-3D model (elevation 1,335 m) is only visualized in part of the domain, since lines 7 to 9 are located at lower elevations and corresponds to the boundary region between the base of the tailings pile and the bedrock (Fig. 11). The direction of the underground flow is well marked by the dispersion of the saline effluent. By correlating the topographic elevations of the study area with the distribution of the low resistivity anomalies, it is possible to infer that the direction of groundwater flow is from southwest to northeast, in line with the natural local drainage pattern. It can also be seen that the contamination plume flows under the old BNF catchment. The three-dimensional models suggest that the acid water plume originates in the intermediate regions of BF-04, at an elevation of 1335 m, in the southeastern portion of the model, and continues at deeper levels, beyond the base of the tailings pile.

In view of this, it can be inferred that groundwater from BF-04 is spreading through fractures in the crystalline basement. The 1300 m level reveals a clear record of the migration of effluents towards the northeast of the study area, with the emergence of a groundwater flow in the SW-NE direction, evidenced by electrical resistivity values of ≈30 Ω·m, as indicated by the model's arrow diagram. It is therefore possible to see that acidic water is being carried beyond the mine's premises through the fracture system. In this way, the water that percolates through the interior of BF-04 acts as a contaminant transport agent for the deep aquifer. As a result, the contaminated effluent seeps into the deeper portions of the regional aquifer

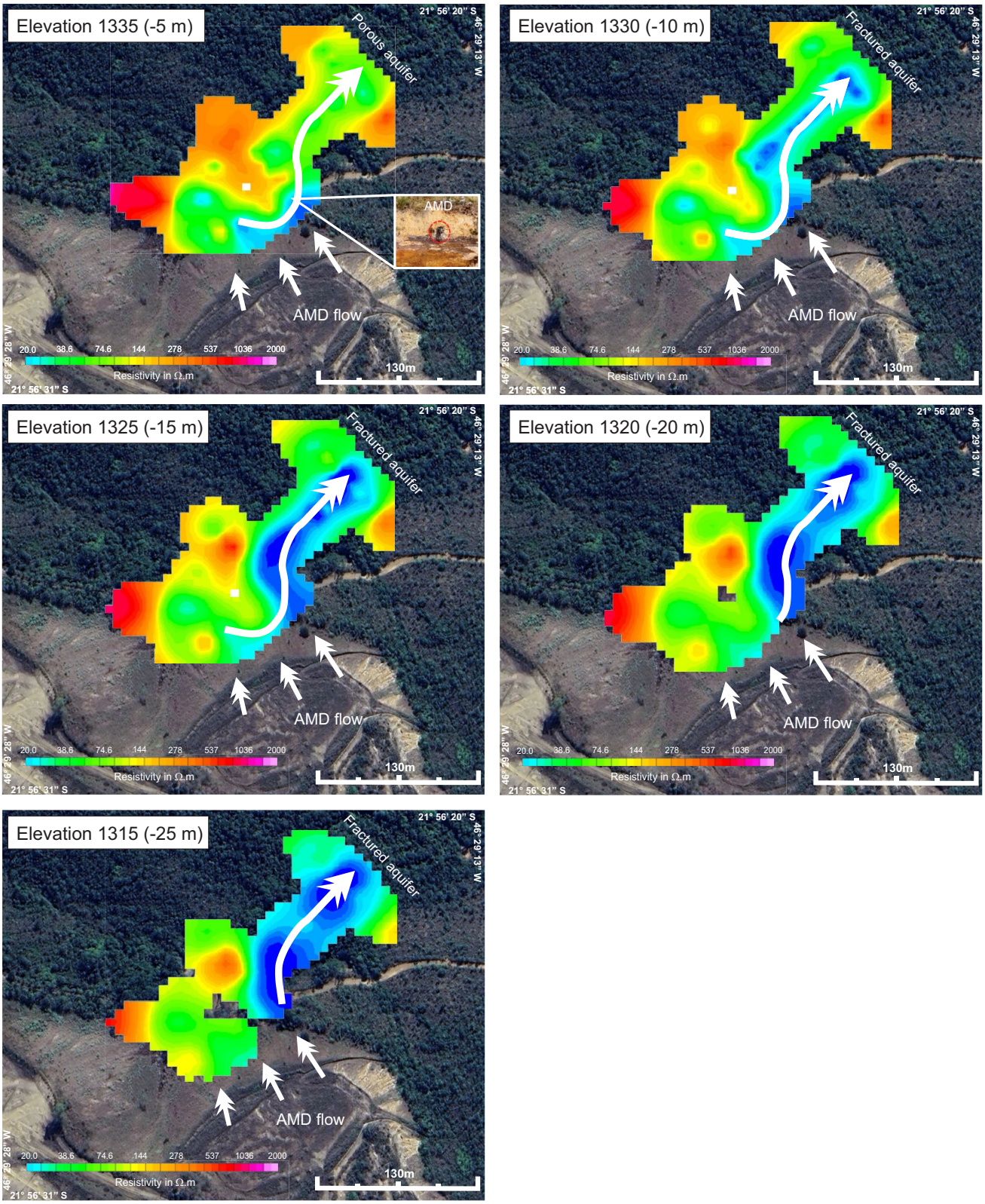

Fig. 11 Maps of electrical resistivity at different depths, spaced at 5 m intervals, generated from 3D visualization models. Detailing the behavior of the more conductive electrical anomaly in the subsurface, suggesting infiltration of AMD from the mining waste pile (white arrow in the depth cross-sections)

through the local fracture system, directly interfering with the quality of the local groundwater (Fig. 11).

Conclusions

The ERT surveys carried out at the decommissioned uranium mine provided electrical resistivity data that suggest an interpretation of the local hydrogeological dynamics and the underground flow of AMD in two distinct systems: the porous system, made up of the tailings pile, and the fractured system, formed by the underlying crystalline basement. The geoelectric sections obtained revealed conductive electrical anomalies that appear to indicate hydraulic connectivity between the tailings pile and the underlying fractured aquifer through the fractures present in the crystalline basement. The zones of low electrical resistivity, with values below 40 Ω·m, are indicative of AMD, visible even on the slope at the base of the tailings pile. This connectivity facilitates the movement and dispersal of AMD and understanding it is fundamental for managing and mitigating environmental impacts during the mine's decommissioning phase.

Managing the flow of groundwater and the dispersion of contaminants in an area with a complex network of fractures, such as the one identified in the study, presents various challenges and opportunities. The connectivity between fractures creates preferential flow paths that are complex in terms of mapping and monitoring. The continuity of these fractures increases the mobility of contaminants, raising the risk of AMD dispersion beyond the limits of the mine, potentially impacting groundwater and surface water quality. The use of geophysical techniques such as ERT allows for a robust diagnosis of underground flow dynamics, which is essential for planning and implementing remediation measures. Techniques for containing environmental damage, such as the use of limestone in open channels and the implementation of hydraulic barriers with limestone, are based on altering the pH to precipitate soluble metals in the AMD. The installation of these systems must consider the local geological context and the identified flow paths, with emphasis in this case downstream of the water catchment reservoir. The long-term effectiveness of these passive systems requires periodic replacement of the dissolved limestone. These passive treatment systems can be combined with actions to restrict the entry of water into the tailings pile, and in an integrated way mitigate the generation and flow of AMD to create a more sustainable mining decommissioning scenario.

Acknowledgements The authors thank the São Paulo Research Foundation (FAPESP) for financial support (Regular Project 2020/14647-0), the Geology Department of São Paulo State University for the use of the geophysical equipment, and the Brazilian Nuclear Industries for providing access to the study area.

Data availability The data that support the findings of this study are available on request from the corresponding author, Guireli Netto, L.

References

ABEM (2012) Terrameter LS—Instruction manual. ABEM Instrument AB: Sundbyberg

Acosta JA, Martínez-Pagán P, Martínez-Martínez S, Faz Á, Zornoza R, Carmona DM (2014) Assessment of environmental risk of reclaimed mining ponds using geophysics and geochemical techniques. J Geochem Explor 147:80–90. https://doi.org/10.1016/j.gexplo.2014.04.005

Akcil A, Koldas S (2006) Acid mine drainage (AMD): causes, treatment and case studies. J Clean Prod 14(12):1139–1145. https://doi.org/10.1016/j.jclepro.2004.09.006

Alberti HLC (2017) Estudo hidroquímico e isotópico das águas subterrâneas impactadas pela drenagem ácida da mina de urânio – Osamu Utsumi, Planalto de Poços de Caldas (MG). Universidade Estadual de Campinas, Campinas, Thesis (**[in Portuguese]**)

Ali MAH, Mewafy FM, Qian W, Alshehri F, Almadani S, Aldawsri M, Aloufi M, Saleem HA (2023) Mapping leachate pathways in aging mining tailings pond using electrical resistivity tomography. Minerals 13:1437. https://doi.org/10.3390/min13111437

Almeida HD, Gomes Marques MC, Sant'Ovaia H, Moura R, Espinha Marques J (2023) Environmental impact assessment of the subsurface in a former W-Sn mine: integration of geophysical methodologies. Minerals 13(1):55. https://doi.org/10.3390/min13010055

Anterrieu O, Chouteau M, Aubertin M (2010) Geophysical characterization of the large-scale internal structure of a waste rock pile from a hard rock mine. Bull Eng Geol Environ 69:533–548. https://doi.org/10.1007/s10064-010-0264-4

Benyassine EM, Lachhab A, Dekayir A, Parisot JC, Rouai M (2018) An application of electrical resistivity tomography to investigate heavy metals pathways. J Environ Eng Geophys 22(4):315–324. https://doi.org/10.2113/JEEG22.4.315

Binley A (2015) Tools and techniques: DC electrical methods. In: Schubert G (Ed), Treatise on Geophysics, vol 11, 2nd edn, Elsevier. https://doi.org/10.1016/B978-0-444-53802-4.00192-5

Blowes DW, Ptacek CJ, Jambor JL (2003) The geochemistry of acid mine drainage. In: Holland HD, Turekian KK (Eds), Treatise on Geochemistry, Elsevier, Vol 5, pp 149–204

Bowker LN, Chambers DM (2015) The risk, public liability and economics of tailings storage facility failures. Download Risk, Public Liability and Economics of Tailings Storage Facility Failures PDF, Accessed Dec 12, 2023

Bram L, Klemetsrud B (2023) Calcium carbonate in waste flooring for neutralization of acid rock drainage. Mine Water Environ 42:70–77. https://doi.org/10.1007/s10230-023-00926-6

Camarero PL, Moreira CA, Pereira HG (2019) Analysis of the physical integrity of earth dams from electrical resistivity tomography (ERT) in Brazil. Pure Appl Geophys 176:5363–5375. https://doi.org/10.1007/s00024-019-02271-8

Canales RM, Kozlovskaya E, Lunkka J, Guan H, Banks E, Moisio K (2020) Geoelectric interpretation of petrophysical and hydrogeological parameters in reclaimed mine tailings areas. J Appl Geophys 181:104139. https://doi.org/10.1016/j.jappgeo.2020.104139

Capovilla MNGM (2001) Urânio nos hidrotermalitos potássicos ("rocha potássica") da Mina Osamu Utsumi, Complexo Alcalino de Poços de Caldas, MG. Thesis, Instituto de Geociências, Universidade de São Paulo, São Paulo – SP. Urânio nos hidrotermalitos

potássicos (rocha potássica) da mina Osamu Utsumi, Complexo (usp.br), accessed Nov. 12, 2023 [in Portuguese]
Casagrande MFS, Moreira CA, Targa DA (2019) Study of generation and underground flow of acid mine drainage in waste rock pile in an uranium mine using electrical resistivity tomography. Pure Appl Geophys 177:1–19. https://doi.org/10.1007/s00024-019-02351-9
Cipriani M (2002) Mitigação dos impactos sociais e ambientais decorrentes do fechamento definitivo de minas de urânio. Thesis, Universidade Estadual de Campinas, Campinas. Accessed Dec. 12, 2023 at: http://libdigi.unicamp.br/document/?code=vtls000282017 [in Portuguese]
Cortada U, Martinez J, Rey J, Hidalgo C, Sandoval S (2017) Assessment of tailings pond seals using geophysical and hydrochemical techniques. Eng Geol 223:59. https://doi.org/10.1016/j.enggeo.2017.04.024
Cruz WB, Peixoto CA (1991) A evolução química das águas subterrâneas de Poços de Caldas - MG. Braz J Geol 21(1):23–33. https://doi.org/10.25249/0375-7536.19912333
Cunha O, Ribeiro A, Scassioti W, Rodrigues F, Katz J (2015) Implantação de projeto de descontaminação de urânio de águas ácidas da mina da INB em Caldas – MG com resinas de troca iônica. XXVI Encontro Nacional de Tratamento de Minérios e Metalurgia Extrativa Poços de Caldas-MG
Dimech A, Cheng L, Chouteau M, Chambers J, Uhlemann S, Wilkinson P, Meldrum P, Mary B, Fabien-Ouellet G, Isabelle A (2022) A review on applications of time-lapse electrical resistivity tomography over the last 30 years: perspectives for mining waste monitoring. Surv Geophys 43:1699–1759. https://doi.org/10.1007/s10712-022-09731-2
Ellert R (1959) Contribuição à geologia do maciço alcalino de Poços de Caldas. Boletim da Faculdade de Filosofia Ciências e Letras. Universidade De São Paulo Geologia 18:5–60
Epov MI, Yurkevich NV, Bortnikova SB, Karin YG, Saeva OP (2017) Analysis of mine waste by geochemical and geophysical methods (a case study of the mine tailing dump of the Salair ore processing plant). Russ Geol Geophys. https://doi.org/10.1016/j.rgg.2017.11.014
Fagundes JRT, Leite AL, Mello CEF, Gomes RC (2008) Balanço hídrico do bota-fora BF4 da mina de Urânio Osamu Utsumi, como subsídio para projetos de remediação de drenagem ácida. Rev Bras de Recur Hídri v. 13, p. 19–28, Available at: ≤ https://www.abrh.org.br/SGCv3/index.php?PUB=1&ID=15&SUMARIO=180≥. Accessed Nov 20 2023
Fernandes AJ, Rouleau A, Vargas Junior ED (2022) Structural geology applied to fractured aquifer characterization. Available at: Structural Geology Applied to Fractured Aquifer Characterization - The Groundwater Project (gw-project.org) Accessed Nov 10 2023
Fernandes HM, Franklin MR (2001) Assessment of acid rock drainage pollutants release in the uranium mining site of Poços de Caldas—Brazil. J Environ Radioact 54(1):5–25. https://doi.org/10.1016/S0265-931X(00)00163-6
Fernandes HM, Franklin MR, Veiga LH (1998) Acid rock drainage and radiological environmental impacts. a study case of the Uranium mining and milling facilities at Poços de Caldas. Waste Manag 18(3):169–181. https://doi.org/10.1016/S0956-053X(98)00019-1
Fraenkel MO, Santos RC, Loureiro FEVL, Muniz WS (1985) Jazida de urânio no Planalto de Poços de Caldas – Minas Gerais. Principais depósitos minerais do Brasil, v. 1, Recursos Minerais Energéticos, MME, DNPM e CVRD, Brasília, pp. 89–103 [in Portuguese]
Franklin MR (2007) Modelagem numérica do escoamento hidrológico e dos processos geoquímicos aplicados à previsão da drenagem ácida em uma pilha de estéril da mina de urânio de Poços de Caldas – MG. 2007. Thesis, Universidade Federal do Rio de Janeiro, Rio de Janeiro – RJ [in Portuguese]
Gomes de Oliveira VM, Tavares Ribeiro LF, Rosalino da Silva MC (2014) Hydrogeologic characterization of the abandoned mining site of Castelejo, Portugal by VLF-EM & RMT-R geophysical surveying. Geofís Int 53(2):135–151. https://doi.org/10.1016/S0016-7169(14)71496-5
Gorman M, Dzombak D (2018) A review of sustainable mining and resource management: transitioning from the life cycle of the mine to the life cycle of the mineral. Resour Conserv Recycl 137:281–291. https://doi.org/10.1016/j.resconrec.2018.06.001
Gudmundsson A, Gjesdal O, Brenner SL, Fjeldskaar I (2003) Effects of linking up of discontinuities on fracture growth and groundwater transport. Hydrogeol J 11:84–99. https://doi.org/10.1007/s10040-002-0238-0
Guedes VJCB, Borges WR, da Cunha LS, Maciel STR (2023) Characterization of an earth dam in Brazil from seismic refraction tomography and multichannel analysis of surface waves. J Appl Geophys 208:104893. https://doi.org/10.1016/j.jappgeo.2022.104893
Guireli Netto L, Malagutti Filho W, Gandolfo OCB (2020) Detection of seepage paths in small earth dams using the self-potential method (SP). REM–Int Eng J 73(3):303–310. https://doi.org/10.1590/0370-44672018730168
Guireli Netto L, Singha K, Moreira CA, Gandolfo OCB, Albarelli DSNA (2023) Investigation of fractured rock beneath a uranium-tailing storage dam through UAV digital photogrammetry and seismic refraction tomography. Front Earth Sci 11:1281076. https://doi.org/10.3389/feart.2023.1281076
Holmes DC, Pitty AE, Noy DJ (1992) Geomorphological and hydrogeological features of the Poços de Caldas caldera analogue study sites. J Geochem Explor 45:215–247. https://doi.org/10.1016/0375-6742(92)90126-S
Islam K, Murakami S (2021) Global-scale impact analysis of mine tailings dam failures: 1915–2020. Glob Environ Chang 70:102361. https://doi.org/10.1016/j.gloenvcha.2021.102361
Jessop M, Jardani A, Revil A, Kofoed V (2018) Magnetometric resistivity: a new approach and its application to the detection of preferential flow paths in mine waste rock dumps. Geophys J Int 215(1):222–239. https://doi.org/10.1093/gji/ggy275
Koppe JC (2021) Lessons learned from the two major tailings dam accidents in Brazil. Mine Water Environ 40:166–173. https://doi.org/10.1007/s10230-020-00722-6
Lachassagne P, Wyns R, Bérard P, Bruel T, Chéry L, Coutand T, Le Strat P (2001) Exploitation of high-yields in hard-rock aquifers: downscaling methodology combining GIS and multicriteria analysis to delineate field prospecting zones. Groundwater 39(4):568–581. https://doi.org/10.1111/j.1745-6584.2001.tb02345.x
Leite JSM (2010) Previsão de drenagem ácida por meio de testes estáticos do material do bota fora da mina de Osamu Utsumi – Caldas, MG (Thesis) - Universidade Federal de Ouro Preto. Escola de Minas. Departamento de Geologia, Ouro Preto [in Portuguese]
Li Q, Zhang J, Gao J, Huang Z, Zhou H, Duan H, Zhang Z (2022) Preparation of a novel non-burning polyaluminum chloride residue (PACR) compound filler and its phosphate removal mechanisms. Environ Sci Pollut Res 29:1532–1545. https://doi.org/10.1007/s11356-021-15724-2
Li S, Liu B, Nie L, Liu Z, Tian M, Wang S, Su M, Guo Q (2015) Detecting and monitoring of water inrush in tunnels and coal mines using direct current resistivity method: a review. J Rock Mech Geotech Eng 7:469–478. https://doi.org/10.1016/j.jrmge.2015.06.004
Lyu Z, Junrui C, Zengguang X, Qin Y, Cao J (2019) A comprehensive review on reasons for tailings dam failures based on case history. Adv Civ Eng. https://doi.org/10.1155/2019/4159306
Loke MH, Lane JW Jr (2004) Inversion of data from electrical resistivity imaging surveys in water-covered areas. Explor Geophys 35(4):266–271. https://doi.org/10.1071/EG04266

Magno Júnior LB (1985) Osamu Utsumi Mine, Geologic Presentation. Relatório interno NUCLEBRÁS. Rio de Janeiro, RJ. Available at: 17054505.pdf (iaea.org), Accessed 10 Dec 2023

Marques T, Matias MS, Silva EFD, Durães N, Patinha C (2021) Temporal and spatial groundwater contamination assessment using geophysical and hydrochemical methods: the industrial chemical complex of Estarreja (Portugal) case study. Appl Sci 11(15):6732. https://doi.org/10.3390/app11156732

Martínez-Pagán P, Gómez-Ortiz D, Martín-Crespo T, Martín-Velázquez S, Martínez-Segura M (2021) Electrical resistivity imaging applied to tailings ponds: an overview. Mine Water Environ 40:285–297. https://doi.org/10.1007/s10230-020-00741-3

Moreira CA, Lapola MM, Carrara A (2016) Comparative analyzes among electrical resistivity tomography arrangements in the characterization of flow structure in free aquifer. Geofís Int 55(2):119–129

Moreira CA, Casagrande MFS, Büchi FMS, Targa DA (2020) Hydrogeological characterization of a waste rock pile and bedrock affected by acid mine drainage from geophysical survey. SN Appl Sci 2(7):1–12. https://doi.org/10.1007/s42452-020-3021-8

Moreira CA, Guireli Netto L, Camarero PL, Bertuluci FB, Hartwig ME, Domingos R (2022) Application of electrical resistivity tomography (ERT) in uranium mining earth dam. J Geophys Eng 19(6):1265–1279. https://doi.org/10.1093/jge/gxac082

Nascimento MMPF, Moreira CA, Duz BG, Silveira AJT (2022) Geophysical diagnosis of diversion channel infiltration in a uranium waste rock pile. Mine Water Environ 41(3):704–720. https://doi.org/10.1007/s10230-022-00878-3

Nyström E, Kaasalainen H, Alakangas L (2019) Prevention of sulfide oxidation in waste rock by the addition of lime kiln dust. Environ Sci Pollut Res 26:25945–25957. https://doi.org/10.1007/s11356-019-05846-z

Nordstrom DK, Blowes DW, Ptacek CJ (2015) Hydrogeochemistry and microbiology of mine drainage: an update. Appl Geochem 57:3–16. https://doi.org/10.1016/j.apgeochem.2015.02.008

Nordstrom DK (2015) Baseline and premining geochemical characterization of mined sites. Appl Geochem 57:17–34. https://doi.org/10.1016/j.apgeochem.2014.12.010

Oliveira M, Moreira CA, Guireli Netto L, Nascimento M, Sampaio B (2022) Geophysical and geological surveys to understand the hydrogeological behavior in an outcrop area of the Guarani Aquifer System, in Brazil. Environ Chall 6:100448. https://doi.org/10.1016/j.envc.2022.100448

Owen JR, Kemp D, Lèbre É, Svobodova K, Murillo GP (2020) Catastrophic tailings dam failures and disaster risk disclosure. Int J Disaster Risk Reduct 42:101361. https://doi.org/10.1016/j.ijdrr.2019.101361

Owen JR, Kemp D, Lechner AM, Ern MAL, Lèbre E, Mudd GM, Macklin MG, Saputra MRU, Witra T, Bebbington A (2024) Increasing mine waste will induce land cover change that results in ecological degradation and human displacement. J Environ Manage 351:119691. https://doi.org/10.1016/j.jenvman.2023.119691

Pelisam LGT (2020) Extração de elementos terras raras e urânio da pilha de minério bota-fora 4 da mina de Osamu Utsumi, utilizando água desionizada, drenagem ácida de mina e ácido clorídrico. Thesis, Universidade Estadual de Campinas, Campinas [in Portuguese]

Placencia-Gómez E, Parviainen A, Hokkanen T, Loukola-Ruskeeniemi K (2010) Integrated geophysical and geochemical study on AMD generation at the Haveri Au–Cu mine tailings, SW Finland. Environ Earth Sci 61:1435–1447. https://doi.org/10.1007/s12665-010-0459-9

Poisson J, Chouteau M, Aubertin M, Campos D (2009) Geophysical experiments to image the shallow internal structure and the moisture distribution of a mine waste rock pile. J Appl Geophys 67(2):179–192. https://doi.org/10.1016/j.jappgeo.2008.10.011

Reynolds JM (2011) An Introduction to Applied and Environmental Geophysics. John Wiley & Sons. An Introduction to Applied and Environmental Geophysics, 2nd Edition | Wiley Accessed Dec 15 2023.

Schoenberger E (2016) Environmentally sustainable mining: the case of tailings storage facilities. Resour Policy 49:119–128. https://doi.org/10.1016/j.resourpol.2016.04.009

Schorscher HD, Shea ME (1992) The regional geology of the Poços de Caldas alcaline complex: mineralogy and geochemistry of selected nepheline syenites and phonolites. J Geochem Explor 45:25–51. https://doi.org/10.1016/0375-6742(92)90121-N

Simate GS, Ndlovu S (2014) Acid mine drainage: challenges and opportunities. J Environ Chem Eng 2(3):1785–1803. https://doi.org/10.1016/j.jece.2014.07.021

Singha K, DayLewis FD, Johnson T, Slater LD (2015) Advances in interpretation of subsurface processes with time-lapse electrical imaging. Hydrol Process 29:1549–1576. https://doi.org/10.1002/hyp.10280

Souza AM, Silveira CS, Pereira RM (2013) Contribuições dos metais provenientes das pilhas de rejeito da Mina Osamu Utsumi a drenagens do Complexo Alcalino de Poços de Caldas. Minas Gerais Geochimica Brasiliensis 27(1):63–76 (**[in Portuguese]**)

Targa DA, Moreira CA, Camarero PL, Casagrande MFS, Alberti HL (2019) Structural analysis and geophysical survey for hydrogeological diagnosis in uranium mine, Poços de Caldas (Brazil). SN Appl Sci 1:1–12. https://doi.org/10.1007/s42452-019-0309-7

Thedeschi MF, Vieira PLNCR, Nomo TA (2015) Projeto fronteiras de Minas Gerais: Folha Caldas/Poços de Caldas, escala 1:100.000. Universidade Federal de Minas Gerais

Ulbrich HH, Vlach R, Ulbrich MN, Kawashita K (2002) Penecontemporaneous syenitic-phonolitic and basic-ultrabasiccarbonatitic rocks at the Poços de Caldas Alkaline Massif, SE Brazil: geologic and geochronologic evidence. Rev Bras Geociênc 32(1):15–26

Waber N (1992) The supergene thorium and rare-earth element deposit at Morro do Ferro, Poços de Caldas, Minas Gerais, Brazil. J Geochem Explor 45:113–157. https://doi.org/10.1016/0375-6742(92)90123-P

Ward SH (1990) Resistivity and Induced Polarization Methods. In: Ward SH (Ed.), Ch. 6, Investigations in Geophysics, pp 147–190. https://doi.org/10.1190/1.9781560802785.ch6

Worlanyo AS, Li J (2021) Evaluating the environmental and economic impact of mining for post-mined land restoration and land-use: a review. J Environ Manag. https://doi.org/10.1016/j.jenvman.2020.111623

Zalán PV, Oliveira JA (2005) Origem e evolução estrutural do Sistema de Riftes Cenozóicos do Sudeste do Brasil. Boletim De Geociências Da PETROBRAS 13(2):269–300